AD-A105 554 NAVAL OCEAN SYSTEMS CENTER SAN DIEGO CA F/G 20/1
WAVE STRUCTURE DETECTION THROUGH TWO-DIMENSIONAL FILTERING.(U)
JAN 81 C MIRABILE
UNCLASSIFIED NOSC/TR-694 NL

END
DATE FILMED
11-81
DTIC

NOSC

NOSC TR 694

NOSC TR 694

Technical Report 694

WAVE STRUCTURE DETECTION THROUGH TWO-DIMENSIONAL FILTERING

C Mirabile

10 January 1981

Final Report: 1 July 1980 to 30 September 1980

Prepared for
Naval Sea Systems Command
Washington, DC 20360

Approved for public release; distribution unlimited

A

NAVAL OCEAN SYSTEMS CENTER
SAN DIEGO, CALIFORNIA 92152

81 10 15

NAVAL OCEAN SYSTEMS CENTER, SAN DIEGO, CA 92152

AN ACTIVITY OF THE NAVAL MATERIAL COMMAND

SL GUILLE, CAPT, USN
Commander

HL BLOOD
Technical Director

ADMINISTRATIVE INFORMATION

Work was accomplished under NAVMAT RTD & EN, 62711N, ZF11-111-003 during the period 1 July 1980 to 30 September 1980. Sponsor was Naval Sea Systems Command (NSEA63R).

Released by
RR Smith, Head
Signal Processing and
Display Division

Under authority of
HA Schenck, Head
Undersea Surveillance Department

UNCLASSIFIED

SECURITY CLASSIFICATION OF THIS PAGE *(When Data Entered)*

REPORT DOCUMENTATION PAGE

READ INSTRUCTIONS BEFORE COMPLETING FORM

1. REPORT NUMBER: NOSC Technical Report 694 (TR 694)	2. GOVT ACCESSION NO.: AD-A105 554
3. RECIPIENT'S CATALOG NUMBER:	
4. TITLE *(and Subtitle)*: WAVE STRUCTURE DETECTION THROUGH TWO-DIMENSIONAL FILTERING	5. TYPE OF REPORT & PERIOD COVERED: Final 1 July 1980 – 30 September 1980
	6. PERFORMING ORG. REPORT NUMBER:
7. AUTHOR(s): C. Mirabile	8. CONTRACT OR GRANT NUMBER(s):
9. PERFORMING ORGANIZATION NAME AND ADDRESS: Naval Ocean Systems Center, San Diego, CA 92152	10. PROGRAM ELEMENT, PROJECT, TASK AREA & WORK UNIT NUMBERS: 62711N, ZF11-111-003
11. CONTROLLING OFFICE NAME AND ADDRESS: Naval Sea Systems Command, Washington, DC 20360	12. REPORT DATE: 10 January 1981
	13. NUMBER OF PAGES: 21
14. MONITORING AGENCY NAME & ADDRESS *(if different from Controlling Office)*	15. SECURITY CLASS. *(of this report)*: Unclassified
	15a. DECLASSIFICATION/DOWNGRADING SCHEDULE

16. DISTRIBUTION STATEMENT *(of this Report)*

Approved for public release; distribution unlimited.

17. DISTRIBUTION STATEMENT *(of the abstract entered in Block 20, if different from Report)*

18. SUPPLEMENTARY NOTES

19. KEY WORDS *(Continue on reverse side if necessary and identify by block number)*

Two-dimensional filtering
Spectrum analysis
Signal processing

20. ABSTRACT *(Continue on reverse side if necessary and identify by block number)*

This report contains an analysis of the potential of using a noncoherent two-dimensional filter technique to extract a ridge-like signal from a two-dimensional surface. The two-dimensional surface consists of the signal plus white Gaussian noise. It is demonstrated that the technique shows promise both in visual ridge detection and in automatic energy ratio detection. It is suggested that a more elegant form of the filter used here (complex coefficient) be used to further enhance the ridge-like signal structure.

DD FORM 1 JAN 73 1473 EDITION OF 1 NOV 65 IS OBSOLETE
S/N 0102-LF-014-6601

UNCLASSIFIED

SECURITY CLASSIFICATION OF THIS PAGE *(When Data Entered)*

SUMMARY

OBJECTIVE

To optimally process surfaces of three-dimensional data to maximize the detection of a ridge-like structure in upper ocean reservation data.

RESULTS

Although based on a very small number of sample points, overall results suggest the structure can be filtered out of noisy data.

RECOMMENDATIONS

Possible directions for further work include:

- o A more elaborate matched filter, possibly using a complex set of filter coefficients, may improve detection performance.
- o Different transforms and mappings may be investigated to put data in different coordinate systems, thereby providing methods to enhance certain structures.
- o Statistics of the energy ratio data should be derived to allow a systematic means for setting the threshold for a specified false alarm rate.

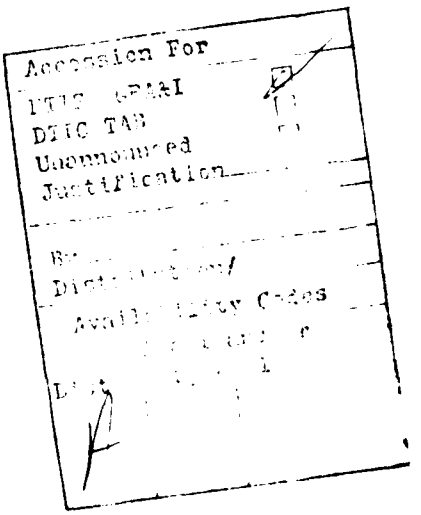

CONTENTS

1.0 INTRODUCTION

The objective of the work documented in this report was to optimally process surfaces of three-dimensional data to maximize the detection of a ridge-like structure in upper ocean reservation data. The source of the active sonar acoustic data was from an experiment performed by the University of California Marine Physical Laboratory (MPL) in 1977. The details and objectives of that experiment are not important to this report. The data were supplied on digital magnetic tape as a time series containing samples from the output of the active sonar receiver. Successive time intervals were time-blocked in the data so that they could be displayed as successive lines of a display as shown in figure 1. Since returns from a wave propagating toward the receiver are received at successively earlier times, the "signal" in this case is perceived as a ridge running diagonally across the data frame.

Processing of this type of data by a matched filter approach was simplified by the fact that detection work for a similar structure was already under way as part of the NOSC Block Program in Long Range Undersea Surveillance. The software to implement a two-dimensional Fourier transform followed by a two-dimensional matched filtering operation was already installed on the Signal Processing Evaluation Laboratory (SPEL) computer system. A strong signal-to-noise ratio case for the present data was used to optimize the parameters of the two-dimensional matched filter.

Previous processing of the MPL data had been accomplished in the two-dimensional domain of figure 1 by convolving a model of the ridge with the data surface. The advantages of the two-dimensional Fourier processing reported here are the flexibility of the filter shape which can be changed to accommodate ridges of different skew, greater computational efficiency, and the establishment of a simple, normalized detection statistic upon which an automatic alert can be based.

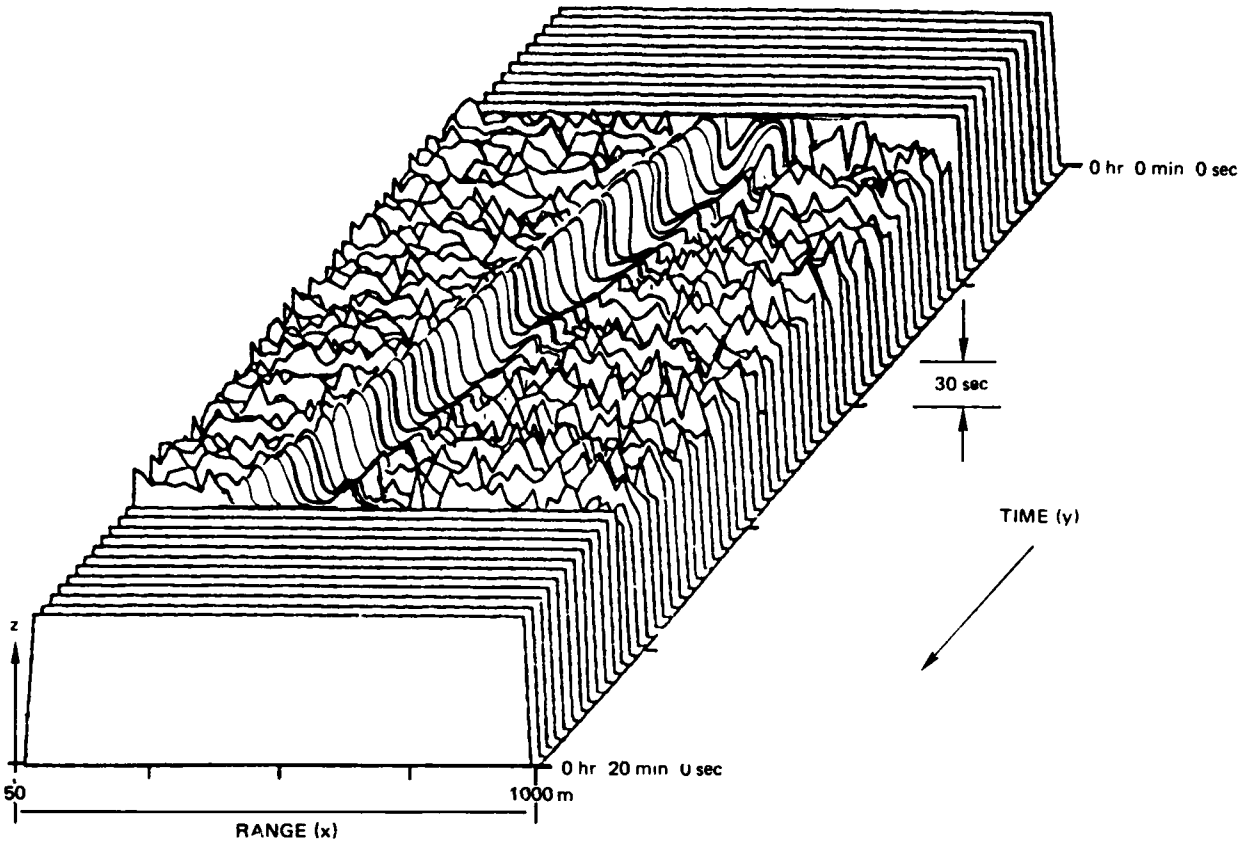

Figure 1. Example of data format with signal wave structure. Successive segments of waveform amplitude vs range are stacked along the time dimension.

The two-dimensional matched filter was as successful, but no more successful, in detecting signal ridges within the data as the previously tried processing. However, as shown in this report, the technique has the potential for an implementation which provides an automatic alert when a ridge structure is present. The skew of the ridge within the data can easily be compensated by a simple change of the two-dimensional filter characteristics. Although the amount of data processed was not sufficient in quantity to establish performance curves for the automatic detection algorithm, the results of this evaluation show that the technique has the potential for automatically detecting the signal structure as an alert within the active sonar system.

In the next section, the data and the two-dimensional filter are described in more detail. The third section contains processed data and analysis results. Finally, the fourth section presents concluding remarks and suggestions for additional work.

2.0 DATA DESCRIPTION AND FILTERING ALGORITHM

Figure 1 shows an example of the active sonar data format from the MPL experiment. It is a three-dimensional graph with range as the x axis and time as the y axis, with time advancing from back to front of the graph. The sample spacing is 30 seconds per line and the z axis is the active sonar receiver amplitude on a linear scale.

A total of ten data segments assumed to contain the M-shaped ridge structure (as in figure 1) were chosen for processing. Also, several sets of data containing different levels of noise were processed. Each data segment, with the exception of the noise data, was approximately one hour in length. For the filtering process, the segments were divided into 20-minute subsegments and processed with a 50% time overlap. The segment numbers, along with the start times of each subsegment, are contained in table 1.

Under the assumption that a signal detection occurs in a white, Gaussian noise background, the optimum filter which maximizes the signal-to-noise ratio is one which matches a replica of the expected signal. In this case, the expected signal is a ridge skewed across the data frame.

The two-dimensional filtering operation can be performed either in the time domain by two-dimensional convolution or in the two-dimensional frequency domain by a multiplication. The frequency domain approach was chosen chiefly

Segment	(Day, Hour, Min)	Segment	Processing Start Time (Day, Hour, Min)
Q T1	13, 20, 45	D14	15, 23, 12
	13, 20, 56		15, 23, 22
	13, 21, 06		15, 23, 32
	13, 21, 16		15, 23, 42
	13, 21, 26		15, 23, 52
T2	13, 22, 01	D15	16, 00, 18
	13, 22, 11		16, 00, 28
	13, 33, 21		16, 00, 38
	13, 22, 31		16, 00, 58
T3	13, 22, 51	D16	16, 00, 18
	13, 23, 01		16, 02, 21
	13, 23,		16, 02, 31
	13, 23, 21		16, 02, 41
	13, 23, 28		16, 02, 51
D6	15, 07, 12	D17	16, 14, 53
	15, 07, 22		16, 15, 03
	15, 07, 32		16, 15, 13
	15, 07, 42		16, 15, 23
	15, 07, 52		16, 15, 33
D13	15, 21, 55	D18	16, 15, 55
	15, 22, 05		16, 16, 05
	15, 22, 15		16, 16, 15
	15, 22, 25		16, 16, 25
	15, 22, 35		16, 16, 35

Table 1. Starting times of the processed subsegments of 20-minute duration and 50% overlap. All graphs which follow are normalized such that 0 minute indicates the first time given in the above segments.

because of its higher computational efficiency. The discrete Fourier transform pair is given by the equations:

$$F(u,v) = \frac{1}{MN} \sum_{x=0}^{M-1} \sum_{y=0}^{N-1} f(x,y)\exp[-i2\pi(ux/M + vy(N)], \qquad 1(a)$$

$$\text{for } u = 0,1,2, \ldots M-1;\ v = 0,1,2, \ldots N-1$$

$$f(x,y) = \sum_{u=0}^{M-1} \sum_{v=0}^{N-1} F(u,v)\exp[i2\pi(ux/M + vy/N)], \qquad 1(b)$$

$$\text{for } x = 0,1,2, \ldots M-1;\ y = 0,1,2, \ldots N-1.$$

The fast Fourier transform (FFT) is normally used to implement equations 1(a) and 1(b).

Figure 2 presents the frequency transfer function and the impulse response of the filter chosen as the model of the expected ridge. The width of the frequency transfer function is narrower toward the center; this allows some variation of the angle of the ridge in the data. The orientation of the filter was obtained using a data frame with very high signal-to-noise ratio (SNR). The width and orientation parameters were varied to obtain the best performance.

3.0 DATA PROCESSING RESULTS

A preliminary look at the spectra for each line of these data showed a very large amount of dc energy. Because of this, the first processing step was to remove the dc so that it could not affect adjacent frequency cells. This was done for each line along the x-axis of figure 1. Processing for the ten data segments of table 1 was then performed according to the following order of operations: FFT, filter, inverse FFT, display.

The detection criterion used initially was visual. For the ten segments processed, very predominant ridge structure was found three times. These data are shown in figures 3, 4, and 5, where the unfiltered data output is on the top and the filtered output is at the bottom. These figures correspond to runs D18, D17, and D6, respectively. In viewing figures 3, 4, and 5, the filtered data are displayed on a magnitude squared amplitude scale and the unfiltered data is on a linear scale.

The ridge in figure 3 is quite strong; in fact, the skewed ridge can be seen in the unfiltered data on close examination. Note that in the unfiltered graphs, twelve lines on either side of the data are set to zero. This zero-padding reduces the effects of circular convolution interference along the time axis. The data are not zero-padded in the x direction because circular convolution effects were found to be small. For comparison, with the strong SNR cases of figures 3, 4, and 5, figure 6 shows the typical filtered and unfiltered data for the case of no ridge detection.

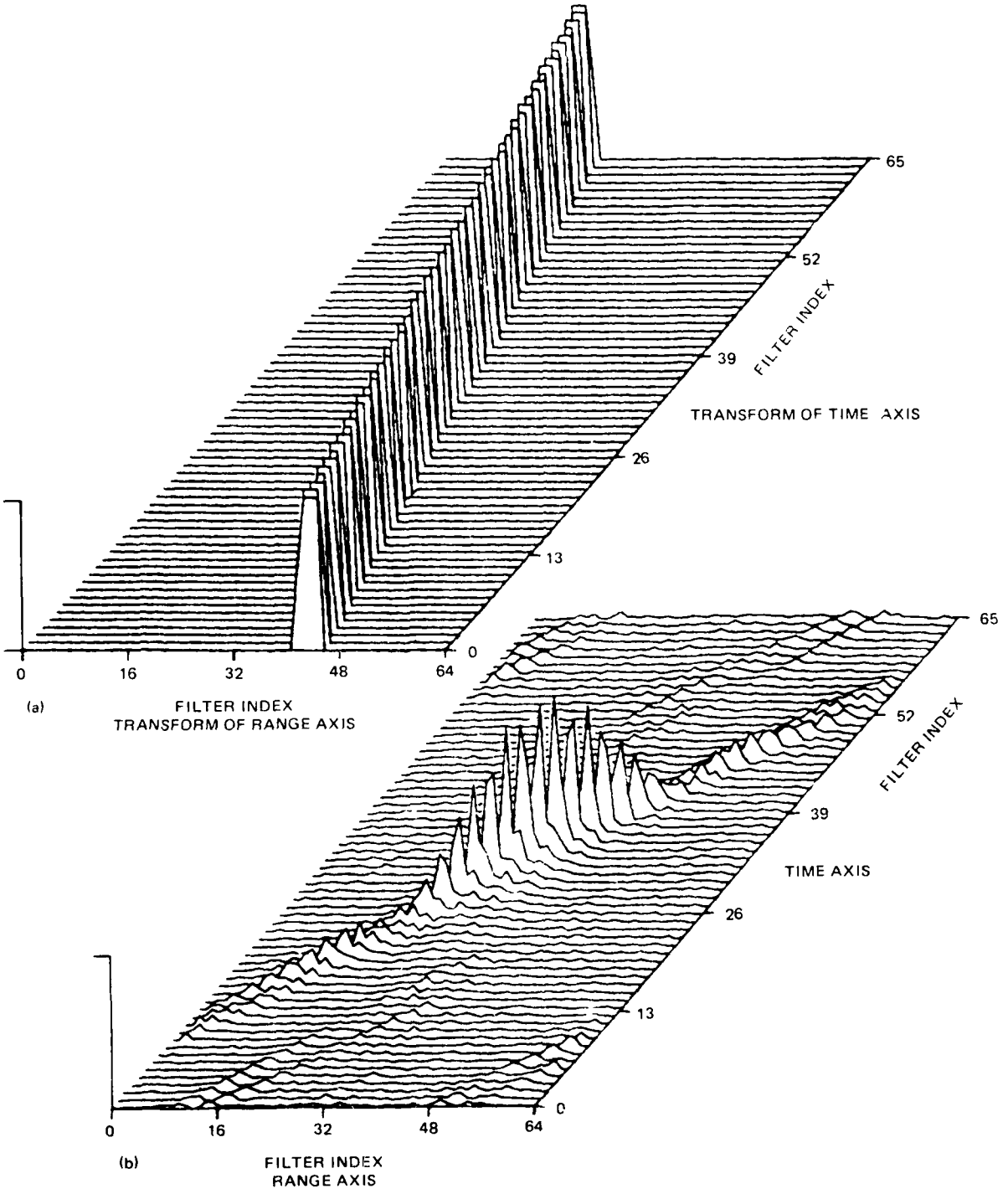

Figure 2. (a) Frequency transfer function and (b) impulse response of the two-dimensional filter. The axes labels are consistent with equations 1(a) and 1(b).

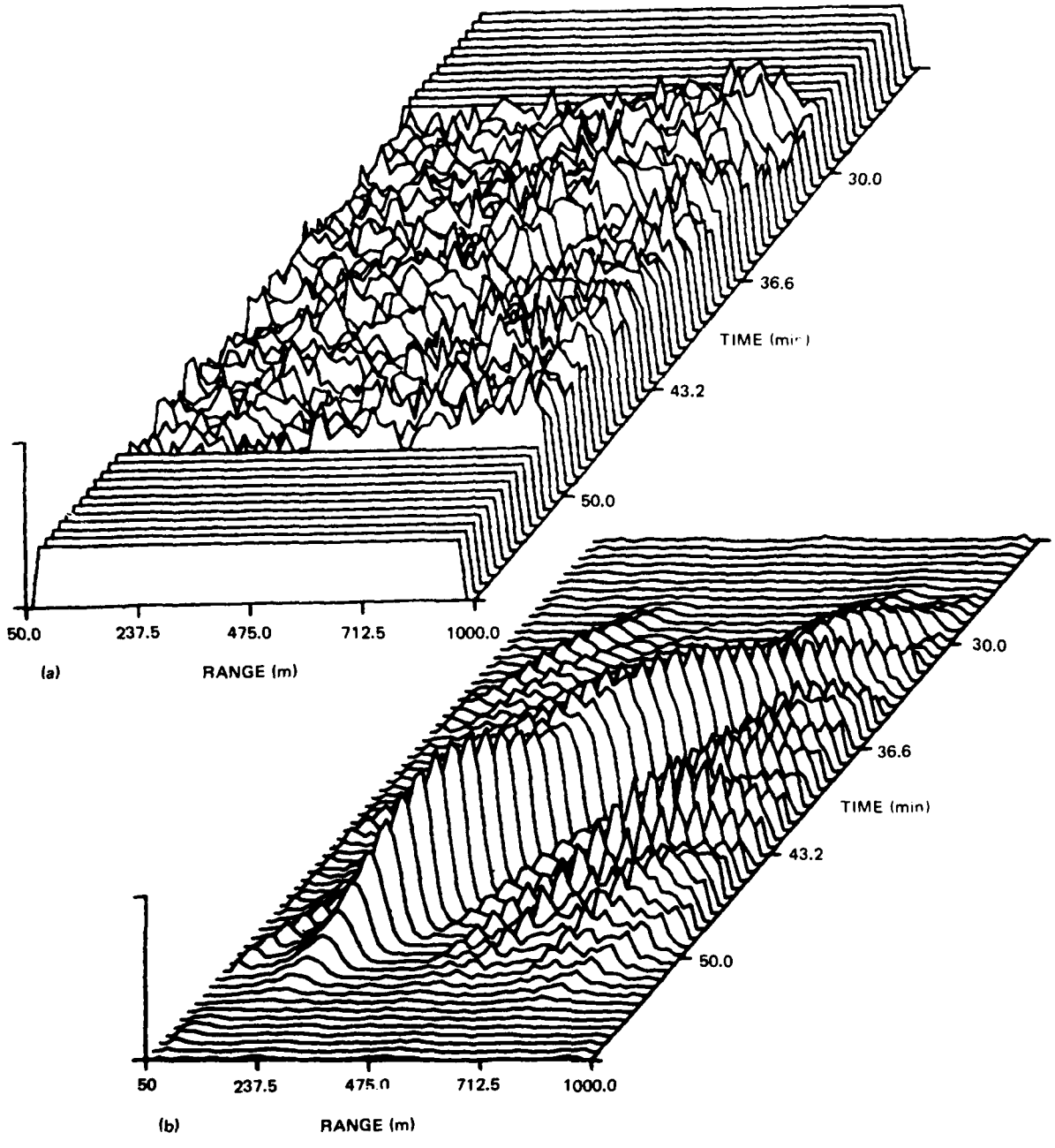

Figure 3. (a) Original unfiltered and (b) filtered data for run D18. The detected ridge is enhanced in the filtered output.

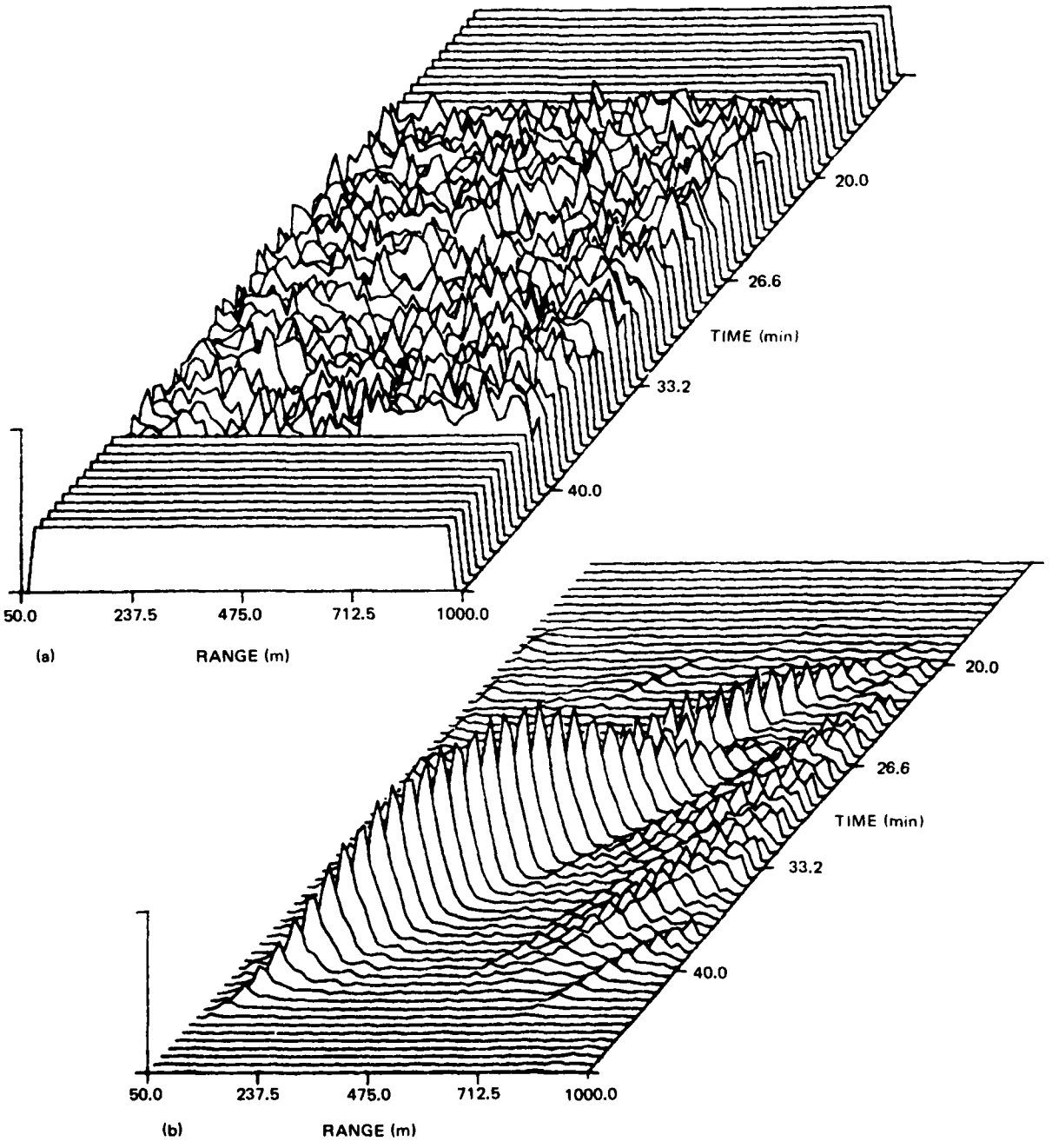

Figure 4. (a) Original unfiltered and (b) filtered data for run D17. The filtered output shows that a ridge has been detected.

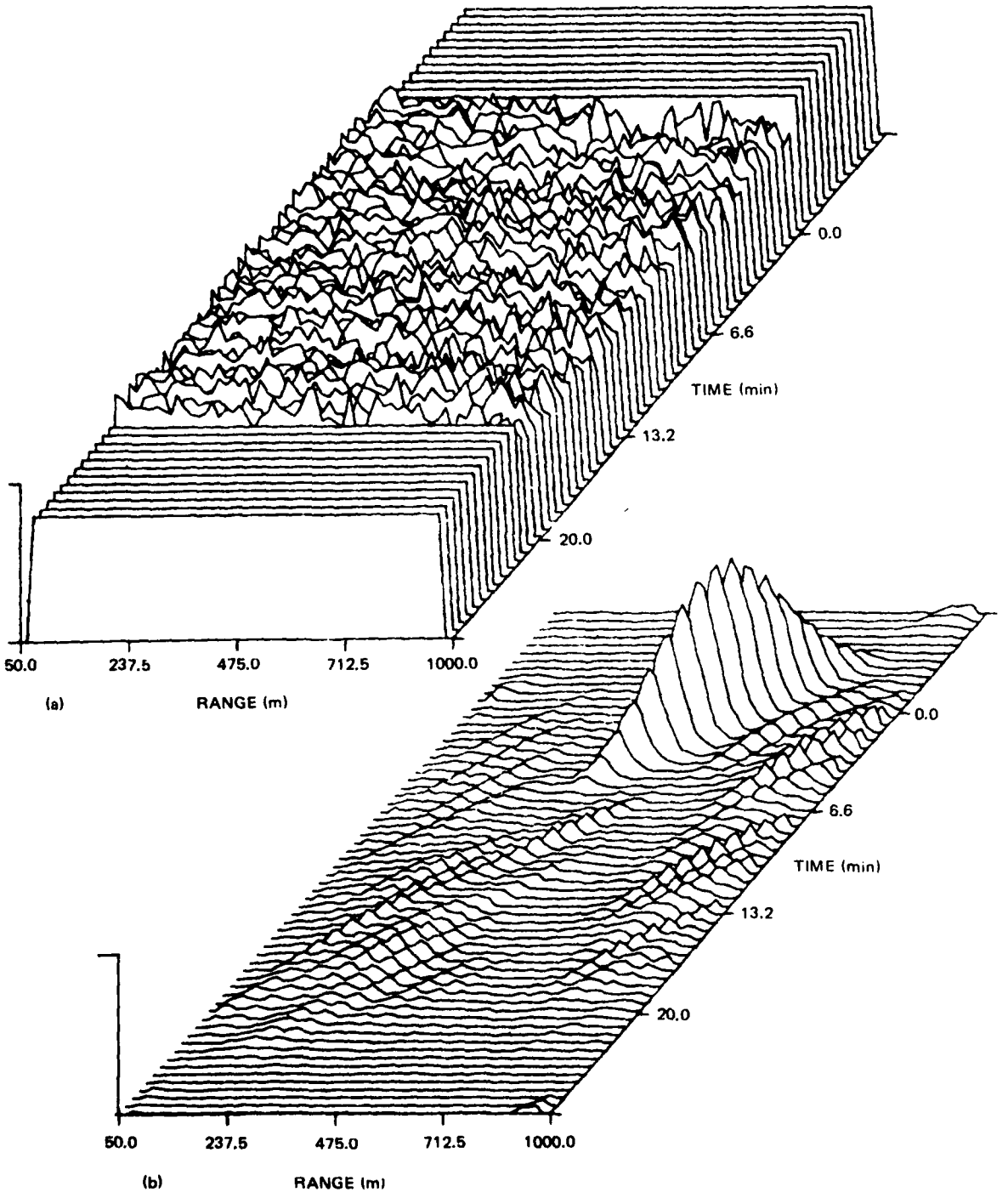

Figure 5. (a) Original unfiltered and (b) filtered data for run D6. The detected ridge did not exist throughout the full range vs time data frame.

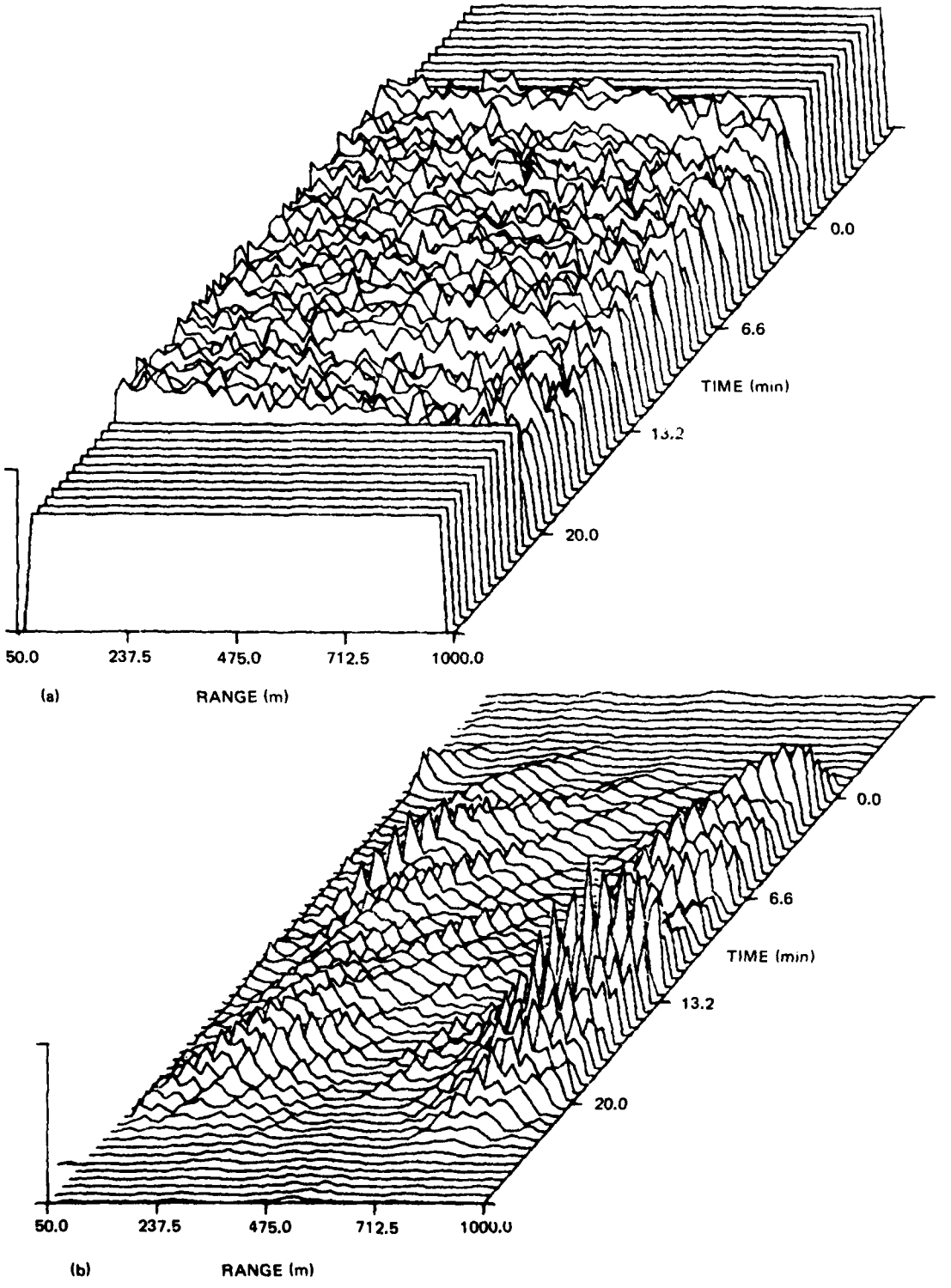

Figure 6. (a) Original unfiltered and (b) filtered data for run T3. No ridge is detectable in this case.

Since the criterion for detection was purely observation of the filtered data plane, the idea of changing the display format was considered. The hidden line display format used thus far has the disadvantage of shadowing some of the high signal spikes. The data from segments D18, D17, and D6 are shown in figures 7, 8, and 9 using a density type format with darker shades indicating higher amplitudes. The subsegments corresponding to the data shown in figures 3, 4, 5 are shown in figures 7, 8, and 9, respectively. Scaling in each segment is based on the maximum value for all subsegments; all five subsegments use this same maximum. The segment containing the data shown in figure 6 is shown in figure 10a (run T3).

There are some interesting points to be made about the graphs. First of all, circular convolution effects can be seen along the x-axis edges of the graphs. The circular convolution can be recognized by a continuation of the right edge of the graph onto the corresponding left edge and vice versa. These edge effects can be seen particularly well in figure 10. Another interesting effect that is noticeable in most of the graphs is particularly discernible in figure 11b (run D15). There are two stationary humps of energy, one at the lower ranges of the graph and one at the higher ranges. In figure 11a, a noticeable ramp-type behavior where total energy increases or decreases in amplitude with range is evident in the data. This ramp appears to change with increasing range in a linear manner. Other data segments showed this same behavior.

In order to confirm that the "ramping" of the data is the cause of the two energy humps, data simulating a ramp were generated and processed through the filter. Figure 12 shows the ramp before filtering and the filtered results; this confirms that the cause of the humps is a ramp underlying the data. The main importance of these humps is that they could mask the ridge structure if the ramp amplitude is large enough.

An effort was made to utilize a detection criterion other than visual for these data. The method selected was to use the ratio of the energy under the filter to the total energy in the subsegment. The assumption is that a higher number represents energy generated from one or more signals. Table 2 shows the energy for all segments processed. The numbers with asterisks denote

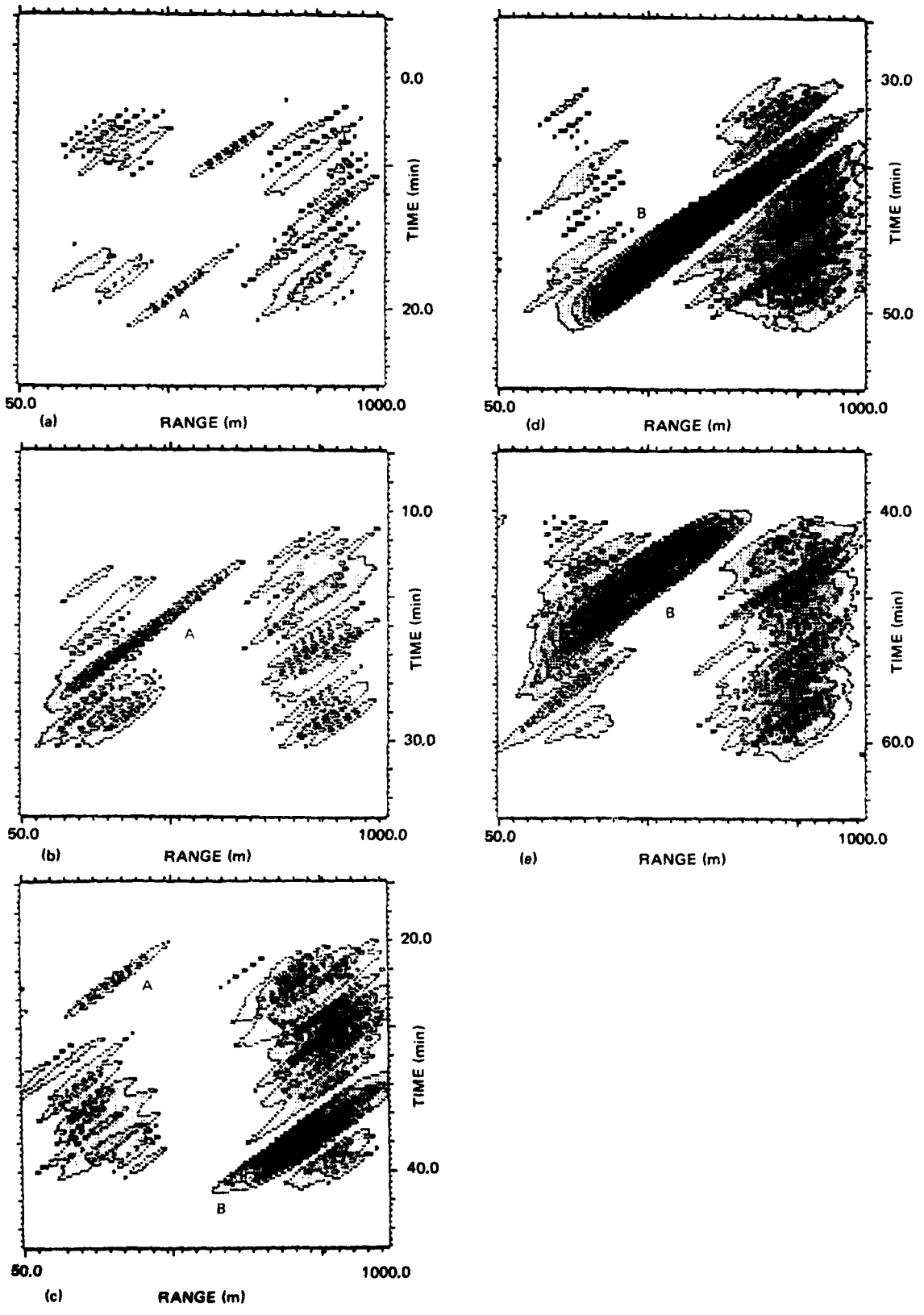

Figure 7. Filtered data for each subsegment of run D18 (figure 3) using a density type display format. Note that there are two ridges detected in these data, labeled A and B on the graphs.

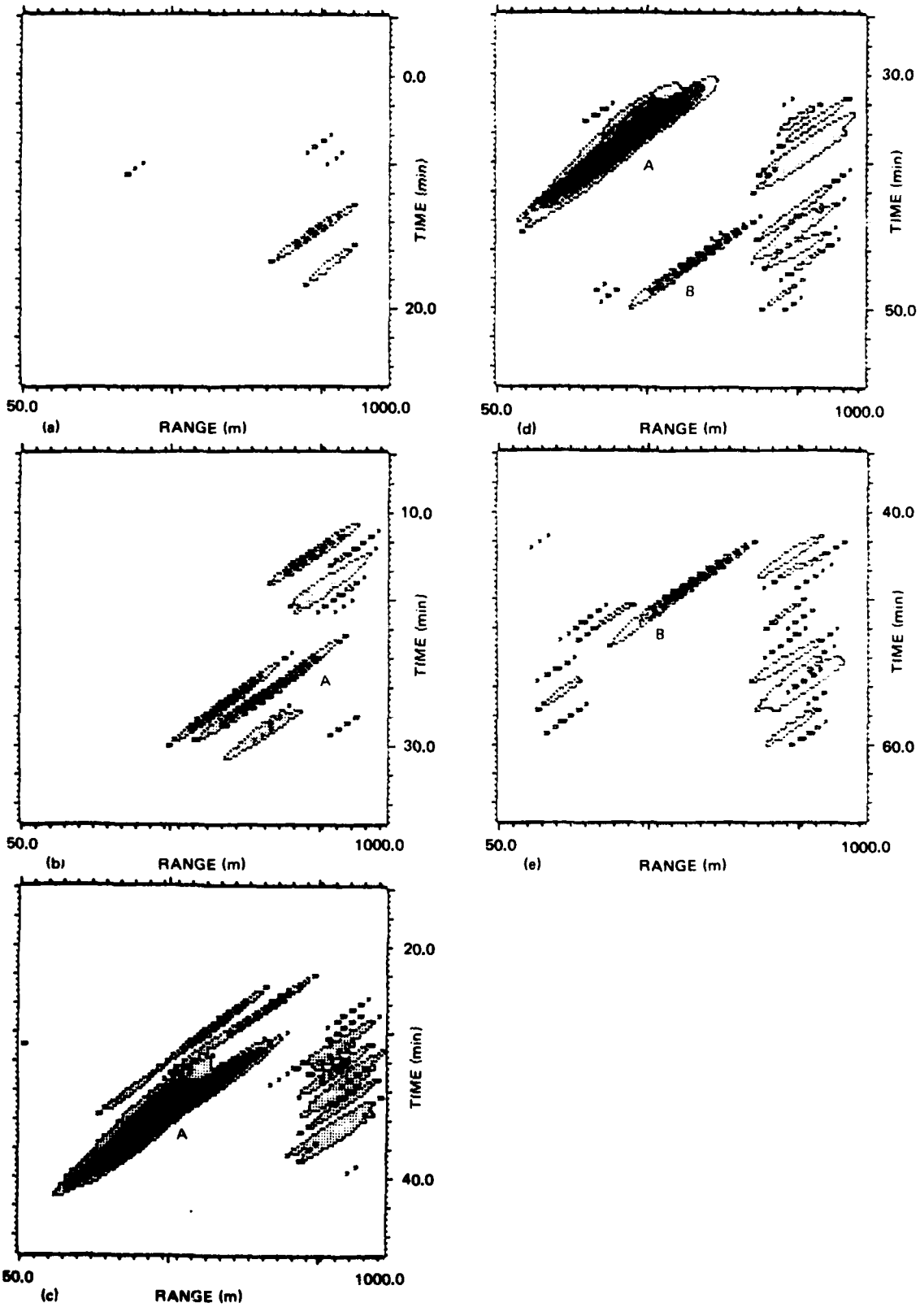

Figure 8. Filtered data for each subsegment of run D17 (figure 4) using a density type display format. Note that there are two detected ridges, labeled A and B.

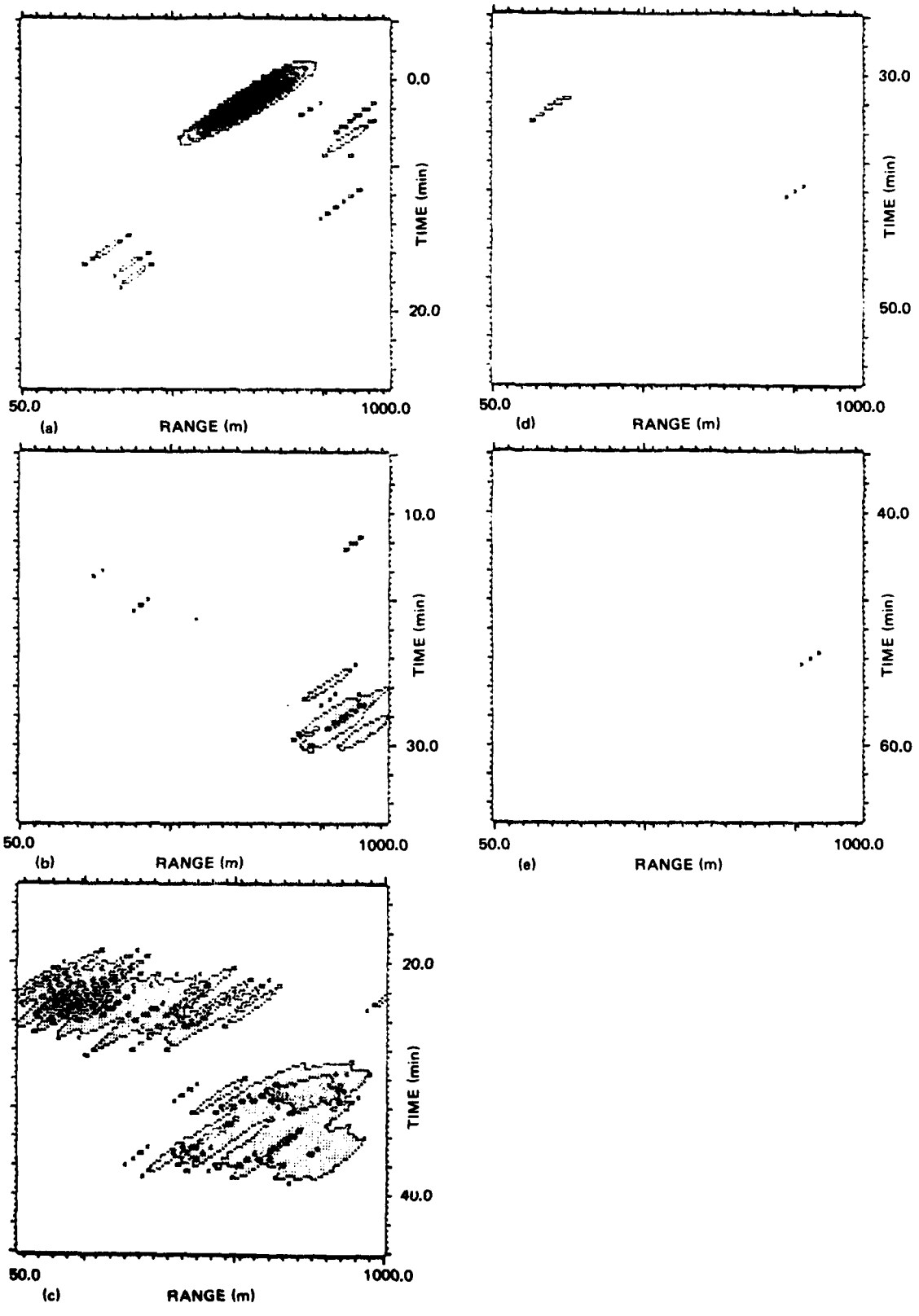

Figure 9. Filtered data for each subsegment of run D6 (figure 5) using a density type display format. A detected ridge is shown in part (a).

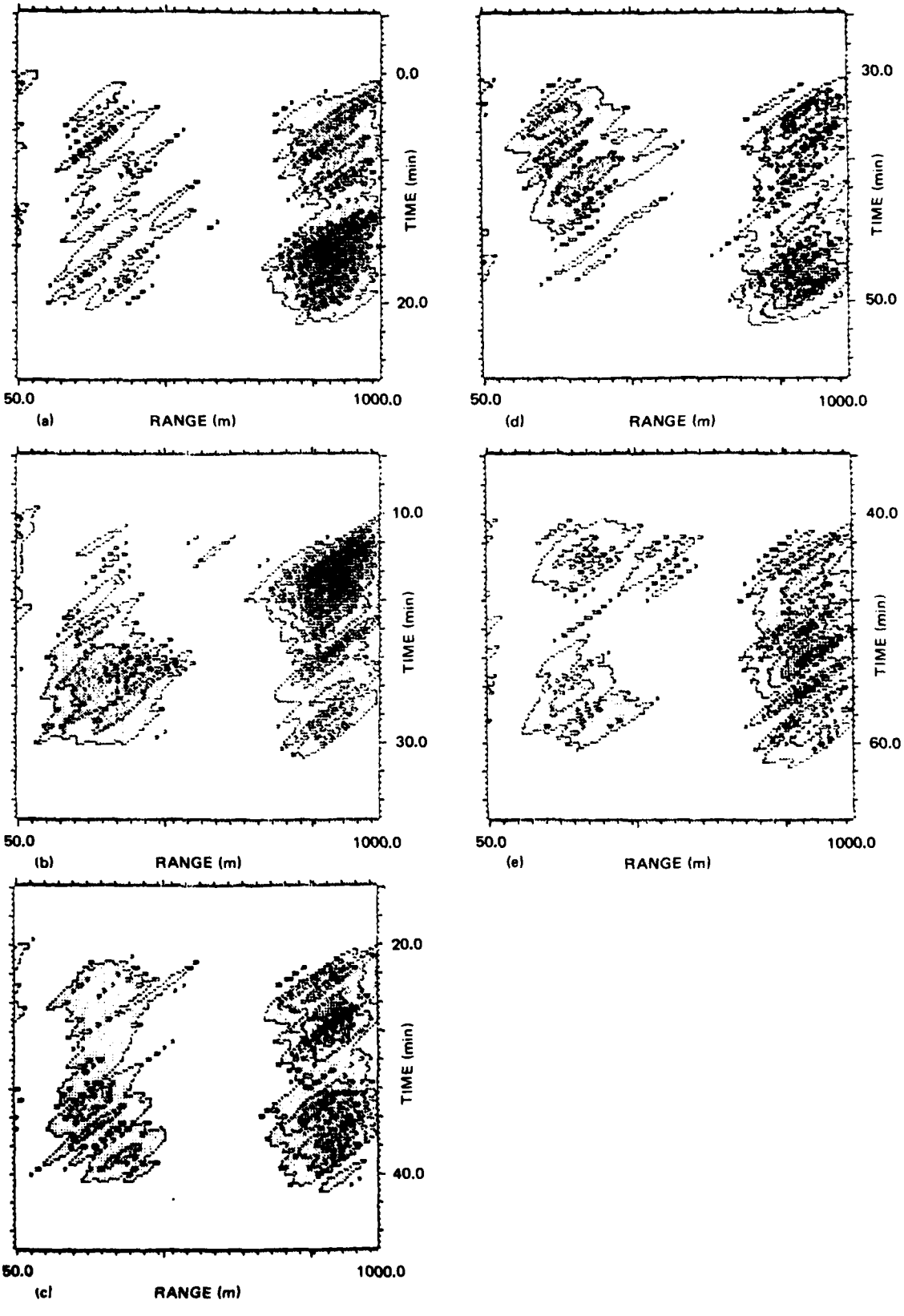

Figure 10. Filtered data for each subsegment of run T3 using a density type display format.

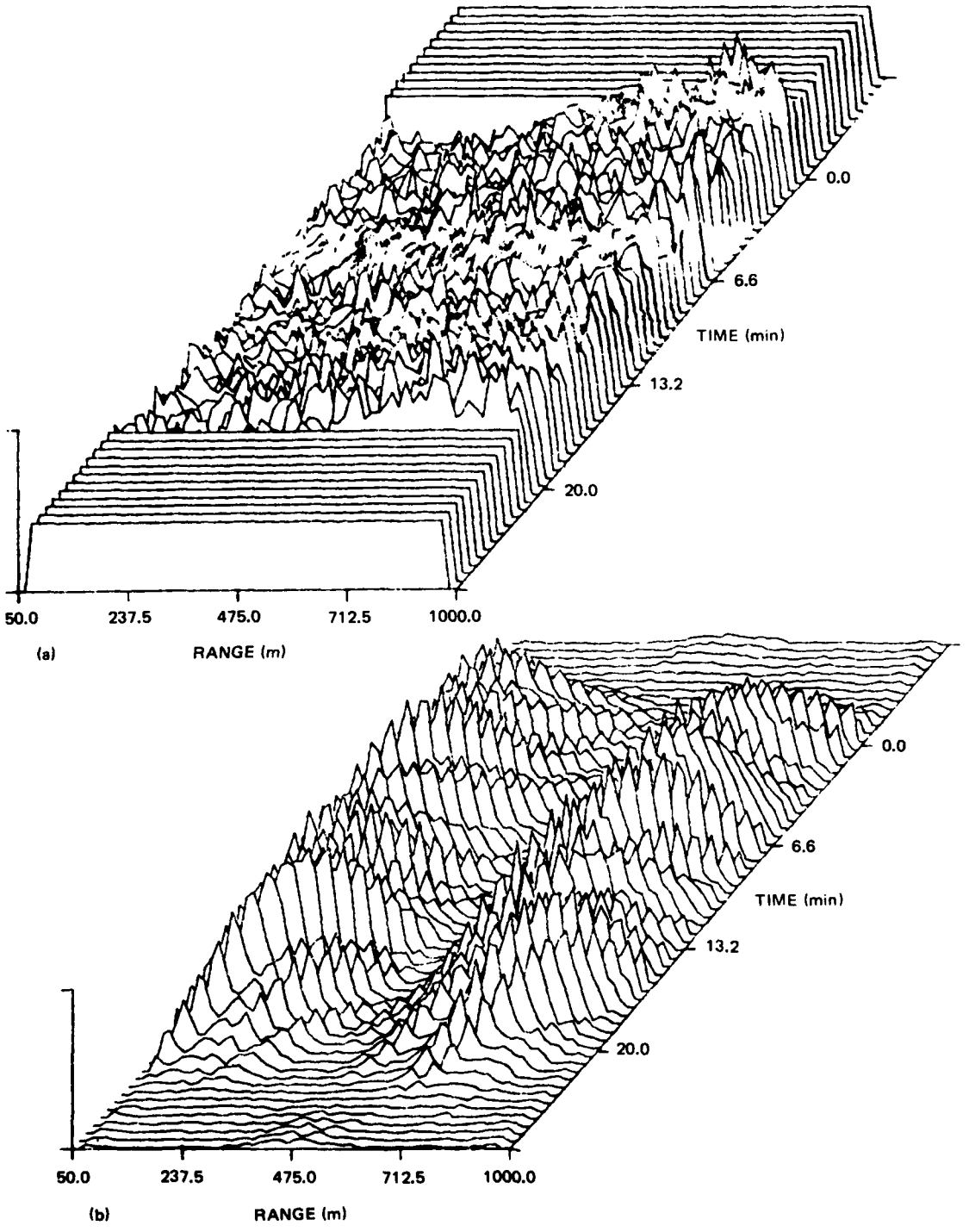

Figure 11. (a) Original unfiltered and (b) filtered data for run D15. Note the two humps of energy to the left and right in part (b).

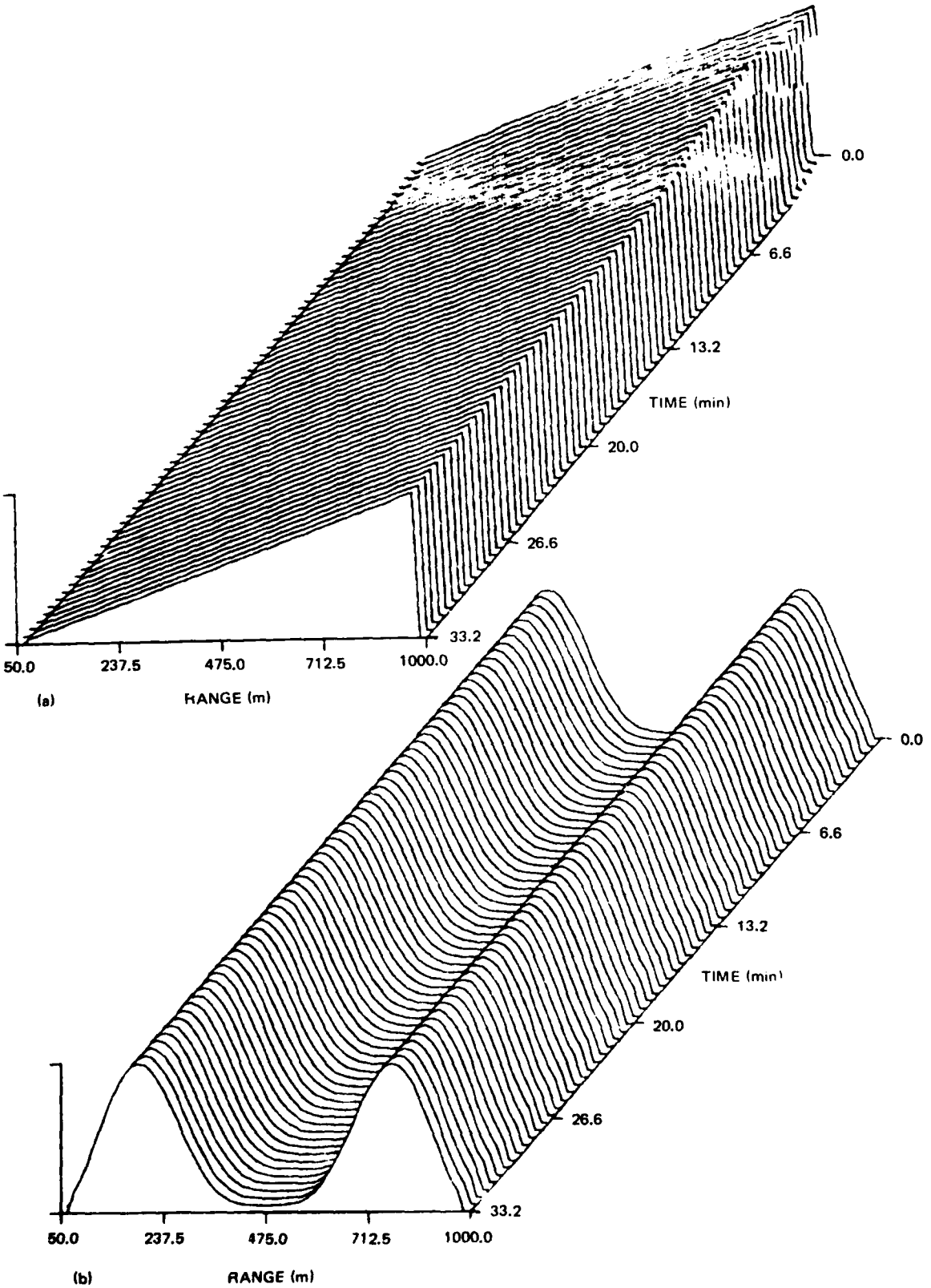

Figure 12. (a) Unfiltered ramp input and (b) filtered data. Note the two humps of energy in (b) due to the ramp signal input of (a).

subsegments where definite ridge structure was seen. It was assumed that a signal could have existed for all the segments, even though visual detections were made only a small number of times. However, "noise only" recordings were made and the same energy ratios computed as for the subsegments assumed to contain a signal. These are listed at the bottom of the table for low, moderate, and high noise level conditions. The noise-only filtered outputs are also shown in figure 13 in a density format.

ENERGY RATIO

SUBSEGMENT RUN	a	b	c	d	e
T1	0.016	0.010	0.016	0.009	0.016
T2	0.011	0.013	0.021	0.018	---
T3	0.018	0.010	0.013	0.023	0.021
D6	0.017*	0.031	0.048	0.039	0.034
D13	0.009	0.013	0.014	0.024	0.019
D14	0.013	0.020	0.019	0.012	0.014
D15	0.021	0.005	0.006	0.023	0.017
D16	0.019	0.017	0.017	0.015	0.012
D17	0.020	0.041	0.035*	0.046*	0.019
D18	0.023	0.014	0.016	0.029*	0.037*

NOISE:		
Low	0.010	
Moderate	0.018	0.029
High	0.024	0.017

Table 2. Energy ratios for each run computed by using the ratio of filtered to total energy for each subsegment. Cases of visual detections are marked by an asterisk. The noise energy ratios were computed under the assumption no signal was present. This was done using subsegments where no disturbance was initiated. Three different noise levels were used.

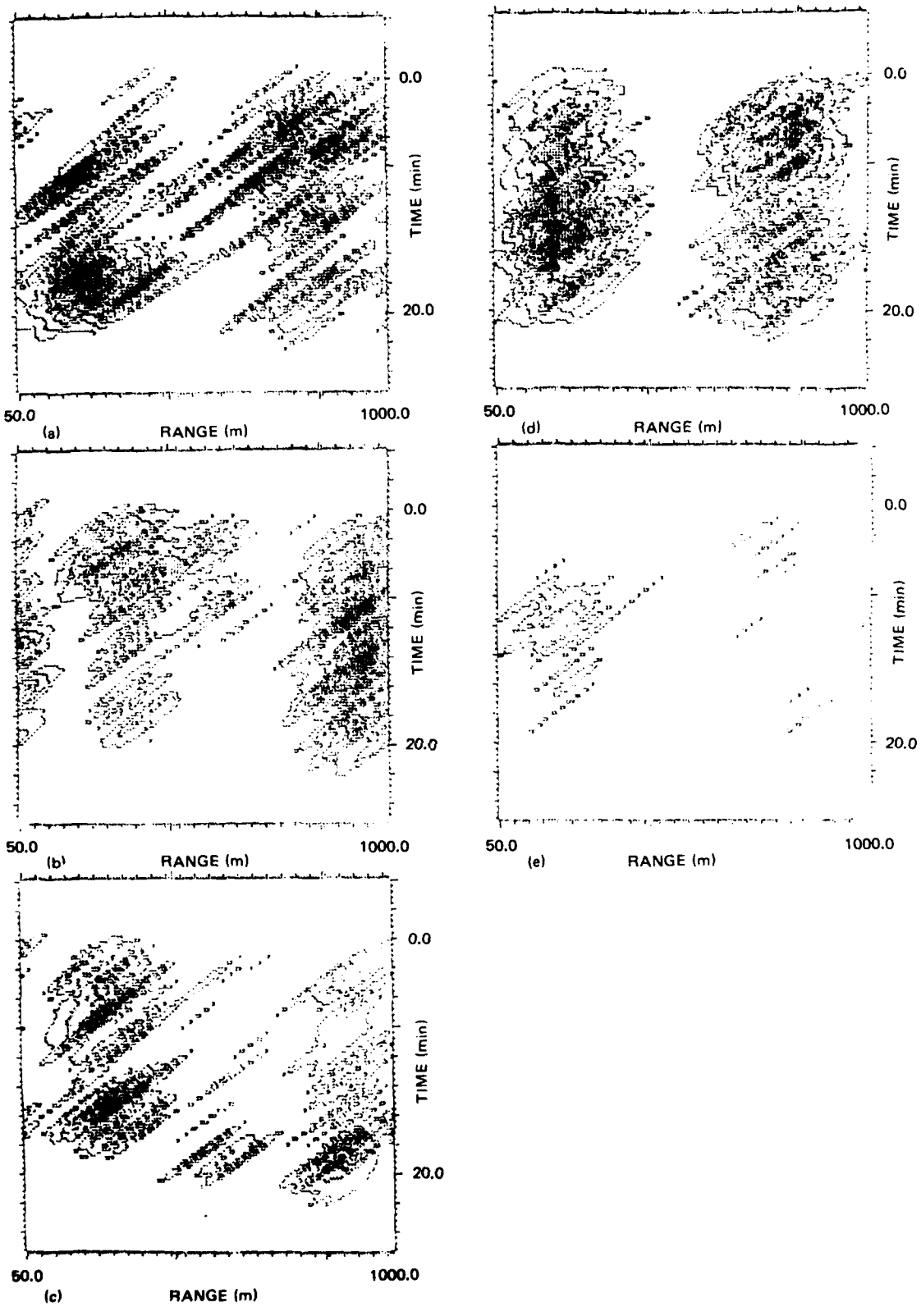

Figure 13. Filtered data for various noise-only inputs. A low noise level is contained in (d), high level in (c) and (e) and moderate level in (a) and (b). Each graph is normalized to its own highest amplitude.

Note from table 2 that the highest values of the energy ratios occur in runs D6, D17, and D18. These correspond to segments where visual detections occurred. However, in the case of run D6, the subsegment where the ridge occurred has a much lower value than the ratios for the rest of the run. It is not obvious from an examination of figure 9 why the final four subsegments of this run have such large ratios.

Some calculations were made to give more perspective to table 2. The mean was computed first for runs T1 through D18 with the exclusion of subsegments with asterisks and second for the noise-only subsegments. These two means were 0.018 and 0.019, respectively. If the 0.018 value is used as a detection threshold over the entire data set in table 2, twenty-seven frames have ratios exceeding the threshold. If the standard deviation is computed and added to the mean, the threshold becomes 0.028 and ten frames exceed that threshold. Finally, going one step farther and eliminating run D6 (which seems to be anomalous), the result is six frames exceeding the threshold of 0.028.

Because of its anomalous behavior, the D6 data were discarded. A histogram of the remaining data is shown in figure 14. Since the data frames were overlapped, we know that if the ridge occurs in subsegment (d) at the middle of the frame it must also occur in subsegments (c) and (e), lower and higher in the frame respectively. For example, if we declare detection in D18 (d), then (c) and (e) must also be put into the signal-plus-noise category. Similarly, for D17, (b), (c), and (d) must be put into the signal-plus-noise category. The portions of the histogram corresponding to these six frames are crosshatched in figure 14.

From figure 14, it can be seen that the crosshatched region is shifted to the right with respect to the rest of the data. This result gives confidence that a false alarm and detection performance could be established as a function of threshold for a larger data set. That is, the filtering technique followed by calculation of the energy ratio has promise for use as an automated detection device for this kind of data because the energy ratio tends to separate the signal-plus-noise case from the noise-only case.

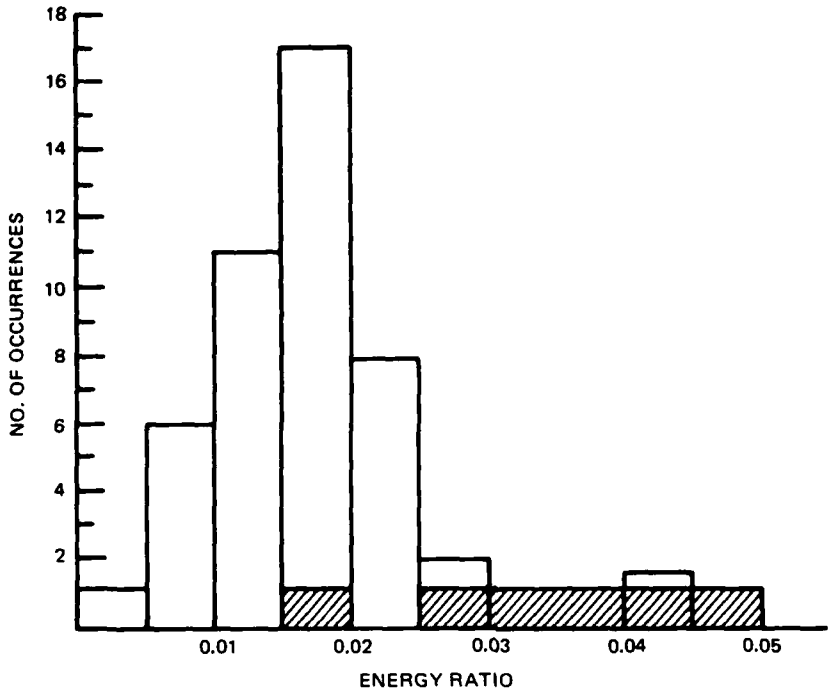

Figure 14. Histogram of the energy ratio data of table 2. Data segment D6 has been excluded because of its anomalous behavior.

4.0 CONCLUSIONS AND RECOMMENDATIONS

The work reported here consists of a brief effort to use a two-dimensional frequency domain filter to filter a signal ridge structure from data. In spite of the fact that the results are based on a very small number of sample points, the overall results suggest that the structure can be filtered out of noisy data.

Some of the most useful results to come from this work are directions for further work. A more elaborate matched filter, possibly using a complex set of filter coefficients, may improve the detection performance. Furthermore, investigation of different transforms and mappings to put the data in different coordinate systems may provide methods which would enhance certain structures. In addition, the statistics of the energy ratio data should be derived to allow a systematic means for setting the threshold for a specified false alarm rate.

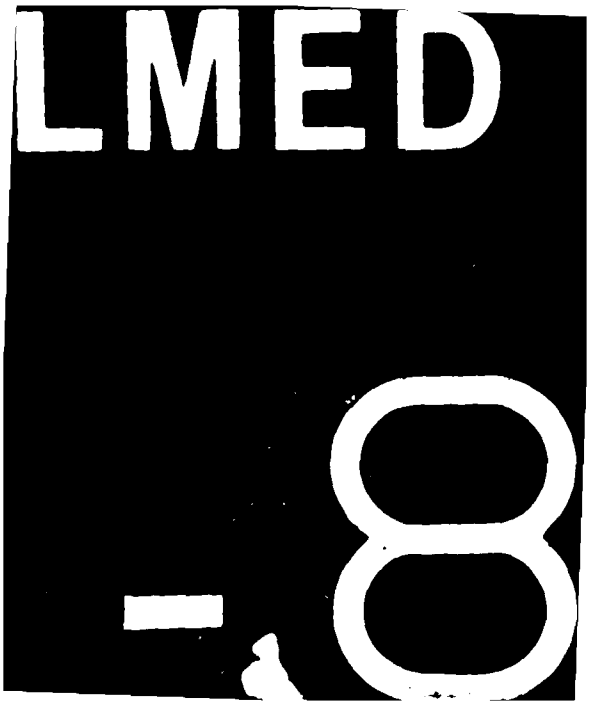
LMED
8